Journal of Dental Sciences 20 (2025) 61–68

Available online at www.sciencedirect.com

ScienceDirect

journal homepage: www.e-jds.com

Original Article

Investigation of the cushioning mechanism of a novel dental implant system with composite hydrogel

Chih-Wen Chi [a], Tze-Wen Chung [b], Yi-Sheng Wu [c], Weng-Pin Chen [c*], Chun-Pin Lin [d,e**]

[a] *Department of Dentistry, National Taiwan University Hospital Hsin-Chu Branch, Hsinchu City, Taiwan*
[b] *Department of Biomedical Engineering, National Yang-Ming Chiao-Tung University, Taipei, Taiwan*
[c] *Department of Mechanical Engineering, National Taipei University of Technology, Taipei, Taiwan*
[d] *Graduate Institute of Clinical Dentistry, School of Dentistry, National Taiwan University and National University Hospital, Taipei, Taiwan*
[e] *National Taiwan University Hospital, National Taiwan University, Taipei, Taiwan*

Received 14 October 2024
Available online 24 October 2024

KEYWORDS
Dental implant;
Composite hydrogel;
Finite element analysis;
Cushioning mechanism

Abstract *Background/purpose:* Dental implants can restore both function and aesthetics in edentulous areas. However, the absence of cushioning mechanical behavior in implants may limit their clinical performance and reduce the long-term survival rates. This study aimed to establish an implant cushion mechanism that mimicked the natural periodontal ligament, utilizing the properties of composite hydrogels.
Materials and methods: In this study, we synthesized two composite hydrogels (HS and HSP groups) using hyaluronic acid (HA) and silk fibroin. We conducted static-constrained compression, creep, and porosity tests to assess the physical properties of these composite hydrogels. Finite element analysis (FEA) was employed to examine the effects of different thicknesses, permeabilities, and compression coefficients on the deformation of the hydrogels. The composite hydrogels were then applied within a novel dental implant, and the displacement performance of the implants, along with stress distribution on the alveolar bone, was evaluated using FEA.
Results: Regarding the mechanical performance of the composite hydrogels, increased permeability led to quicker displacement under compression. Thicker hydrogels with larger compression moduli influenced the biphasic behavior and deformation. The novel dental implants demonstrated biphasic sinking behavior under loading and rapid repositioning during

* Corresponding author. Department of Mechanical Engineering, National Taipei University of Technology, No. 1, Sec. 3, Chung-Hsiao E. Rd., Da-an District, Taipei 10608, Taiwan.
** Corresponding author. Graduate Institute of Clinical Dentistry, School of Dentistry, National Taiwan University, No. 1, Chang-Te Street, Taipei 10048, Taiwan.
E-mail addresses: wpchen@mail.ntut.edu.tw (W.-P. Chen), chunpinlin@gmail.com (C.-P. Lin).

https://doi.org/10.1016/j.jds.2024.10.016

unloading. When evaluating stress distribution on the alveolar bone under oblique loading, the HS and HSP implant groups showed a stress reduction of 10.3 % and 13.6 %, respectively, compared to commercial implant groups.
Conclusion: This study highlights that the biphasic nature of solid and liquid phases is crucial when incorporating a cushioning mechanism into implants to replicate the characteristics of the periodontal ligament.

Introduction

Dental implants offer a reliable clinical solution for missing tooth restoration, enhancing aesthetic and functional outcomes. The long-term survival rate for the dental implants ranges from 83 % to 90 %.[1,2] However, some complications can arise with the extended use of dental implants. The most common complications include peri-implant tissue inflammation, surrounding bone loss, implant body or screw fracture, and implant body loosening.[3–6] Factors contributing to dental implant failure encompass the prolonged wear and tear, inadequate oral hygiene, and occlusal overload.[7]

In natural teeth, the periodontal ligament (PDL) tissue surrounds the root surface, with a thickness ranging from 0.15 mm to 0.38 mm.[8,9] This tissue connects the cementum to the surrounding alveolar bone. When teeth are subjected to functional occlusal forces, the PDL helps support and redistribute these forces evenly across the entire dental arch.[10,11] Previous studies have indicated that the PDL has a unique 'escape' ability, allowing for micromovement of approximately 0.2 mm during biting.[12–14] This movement, influenced by the viscoelastic phenomenon of PDL,[15,16] facilitates equal stress distribution among neighboring teeth and prevents the stress concentration on the alveolar bone. The viscoelastic phenomenon of PDL arises from modeling the fibrous structures[17] and gradually flowing tissue fluid[15] of the PDL. In contrast, current dental implants achieve osseointegration directly with bone tissue, lacking the support of a PDL. As a result, occlusal loading on dental implants can lead to stress concentration in the surrounding bone and the implant itself, which may ultimately result in bone resorption or implant failure.[18] Therefore, the development of a novel implant that could replicate the performance of the PDL would likely enhance clinical outcomes.

Hyaluronic acid (HA) has an anti-parallel double helix structure, where hydrogen bonds formed by the electrostatic forces of carboxyl groups between adjacent sugar rings enhance its stability. HA exhibits excellent biocompatibility and has been used in the cartilage tissue for impact absorption and stabilization of collagen structures.[19] The viscosity and elasticity of HA can be modified based on its concentration, molecular weight, and molecular interactions. Natural silk fibers, devoid of sericin, also demonstrate exceptional biocompatibility and are resistant to degradation. These fibers provide mechanical strength and stability in various biomaterials.[20] The silk fibers have been commonly used in tissue engineering and drug delivery systems.[21]

Finite element analysis (FEA) has yielded significant research findings in the fields of implant design and stress distribution under loading. In recent decades, numerous studies have focused on replicating the PDL phenomenon within dental implants using FEA.[22–25] However, these studies predominantly employed the linear elastic buffering materials and were unable to accurately replicate the biphasic mechanical properties of the PDL. In this study, we combined HA and silk fiber to synthesize a hydrogel composite. This composite was applied to a novel implant to simulate the biphasic movement of natural teeth. Additionally, we investigated the micro-movement of the novel implant under loading conditions through FEA.

Materials and methods

Synthesis of composite hydrogel

The novel composite hydrogel materials were prepared by cross-linking HA with silk fibroin. The preparation involved reacting HA with the cross-linking agent BDDE (1,4-butanediol diglycidyl ether). Silk fibroin was then added to the solution and stirred to complete the reaction. An HCl solution was used to terminate the BDDE cross-linking reaction. Final cross-linking was achieved using EDC/NHS (N-(3-dimethylaminopropyl)-N′-ethyl-carbodiimidehydrochloride/N-hydroxysuccinimide) to enhance the bonding between the carboxyl groups of HA and the amine groups of silk fibroin, resulting in the HS group (Fig. 1a). To further improve the internal bonding of the material, polydopamine was incorporated in the final step, yielding the HSP group (Fig. 1b). Twelve specimens were prepared for each group.

Mechanical properties test for composite hydrogel

In this study, the molds were designed using SolidWorks (SolidWorks Corporation, Boston, MA, USA) and fabricated from acrylic resin. Each mold had an outer diameter of 30 mm, an inner diameter of 3 mm, and a height of 15 mm. A hole with an inner diameter of 25.5 mm and a depth of 2.5 mm was cut at the bottom of the mold to accommodate a 100 μm porous plate, simulating fluid behavior. A cylindrical plunger with a diameter of 3 mm was created to apply pressure to the specimen (Fig. 1c).

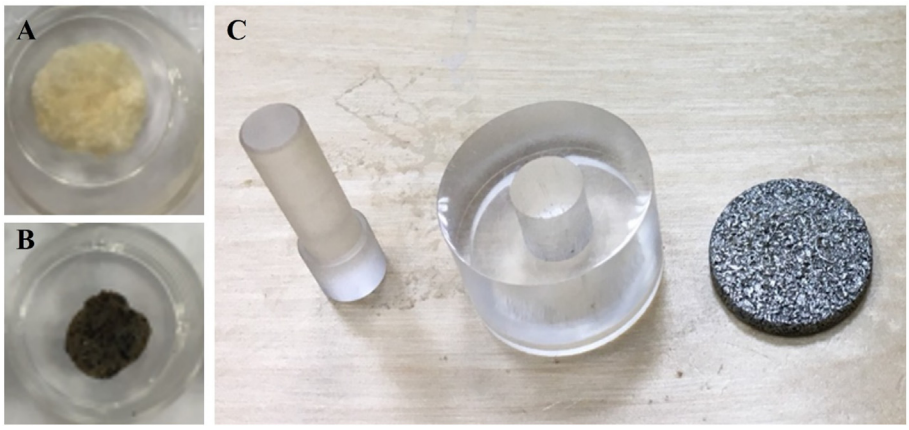

Figure 1 The illustration of the sythesized materials and the experimental models. (A) The HS group sample resulted from hyaluronic acid and silk fibroin combination. (B) The HSP group sample resulted from hyaluronic acid, silk fibroin, and polydopamine combination. (C) Experimental molds for compression test, left: the cylindrical pressure plunger, middle: the closed hollow mold, and right: the porous plate.

The composite hydrogel specimen and porous plate were placed in the mold and soaked within the saline solution. Displacement control was performed on a material testing machine (MTS Bionix 858, MTS Systems Co., Eden Prairie, MN, USA) with a loading condition of 0.2 mm/s until a displacement of 2 mm (50 % strain) was reached. The experimental results the output force–displacement curves. The Young's modulus, E value was calculated using Formula 1.1, and the Poisson's ratio was calculated using Formula 1.2.

$$E = (F/A)/(\delta/L) \tag{1.1}$$

$$\mathrm{Ha} = \mathrm{E}\,(1-\nu)\,/\,[(1+\nu)\times(1-2\times\nu)] \tag{1.2}$$

We applied standard weights (F1 grade - stainless steel standard weights, Honder Weighing Scale Co., Ltd., New Taipei city, Taiwan) on the platform to apply a fixed force and recorded the displacement changes of the specimen with a linear displacement transducer (HR-100, Measurement Specialties Inc., Miamisburg, OH, USA) and displacement display unit (TRACKER 200, Data Track Process Instruments Ltd., Mold, Flintshire, UK).

The experimental procedure followed the method used by *Silva* et al. to measure the porosity ratio of specimen.[26] The wet weight (Wwet) and dry weight (Wdry) of each set of composite hydrogels were measured using an electronic analytical balance (AS/C1, Radwag Balances and Scales, Radom, Poland) to calculate the porosity ratio of the composite hydrogels through Equation (1.3). Firstly, the specimen was freeze-dried in a freeze dryer (Benchtop 2 K, Virtis Comampany Inc., Gardiner, NY, USA) at −50 °C for 24 h to measure its dry weight. Then, their wet weight was measured after soaking the composite hydrogels in water for 1 h.

$$e_0 = V_f\,/\,V_s = ((m_f\,/\,\rho_f))\,/\,(V_T - V_f) \tag{1.3}$$

V_f: liquid volume, V_s represents the solid volume of the tissue, ρ_f represents the liquid density, m_f represents the mass of the liquid ((Wwet - Wdry)/ρ_f), and V_T represents the total volume of the tissue ($V_f + V_s$).

Construction and analysis of composite hydrogel models with FEA

Considering the mechanical behaviors of composite hydrogel with loading, we applied a biphasic linear model as the permeability theory to simulate fluid and solid performances. In order to simulate the change in the elastic properties of the materials with time after loading, this study referred to the relationship (Equation (1.4)) between porosity and permeability proposed by Argoubi and Shirazi-Adl,[27] and the parameters obtained from the experiment, initial permeability (k_0) and initial porosity (e_0), were substituted into this non-linear formula (Equation (1.4)) to obtain the permeability (k) that changes with time. Where M is an experimental parameter, verification was done using the results of creep experiments and FEA.

$$\mathrm{k} = k_0\left[\frac{e(1+e_0)}{e_0(1+e)}\right]^2 exp\left[M\left(\frac{1+e}{1+e_0}\right)-1\right] \tag{1.4}$$

To simulate the mechanical performance of this composite hydrogel, this study adjusted the parameters of the liquid phase permeability, the solid phase compressive modulus, and the thickness of the material (0.3 mm, 0.9 mm, 1.8 mm, and 3 mm) using FEA to analyze the displacement changes of the composite hydrogel during loading and rebound. The analysis was set to apply a 5 N axial load for 1 s and then remove it. The displacement of the material was recorded over time.

FEA of the novel composite hydrogel applied in dental implants

We utilized a conventional ITI implant (Institut Straumann AG, Basel, Switzerland) as a base model. The novel abutment was modified and designed as three components: the internal body, coping, and buffer O-ring (Fig. 2). This design utilized the gap between the internal and external threads, incorporating the buffer to allow for a slight mobility of 0.2 mm in the artificial dental implant, with the buffer

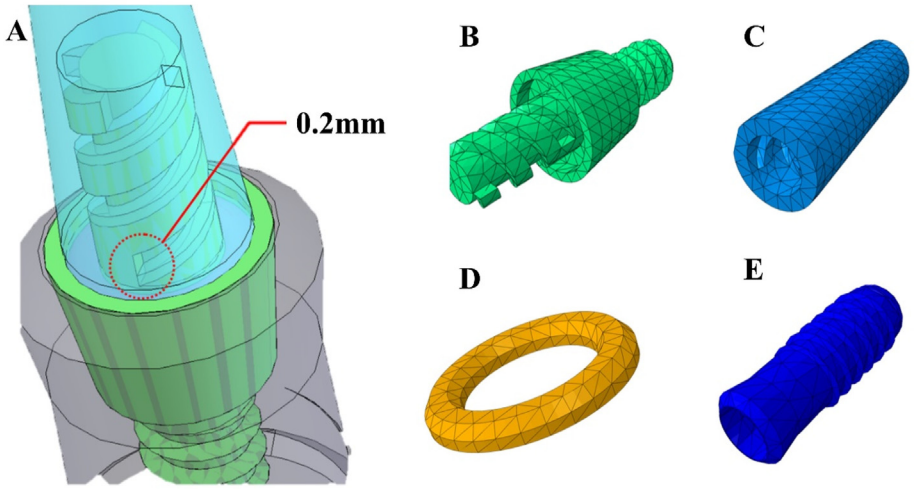

Figure 2 Solid models for the finite element analyses. (A) Illustration of assembling the novel implant with 0.2 mm gap. (B) Internal body of the novel abutment. (C) Coping of an abutment. (D) The hydrogel composite O-ring. (E) The implant body.

material having a thickness of 0.3 mm. The model of the alveolar bone was simplified to a geometric dimension of a block with a height of 20 mm and a length and width of 17 mm. It included a geometric dimension of the cancellous bone in the block with a length and width of 13 mm and a height of 16 mm and a cortical bone with an outer covering thickness of 2 mm. The solid models of two implants were designed using SolidWorks (SolidWorks Co.), and FEA software ABAQUS/CAE (SIMULIA, Dassault Systèmes, Johnston, RI, USA) was used with the ten-node second-order tetrahedral elements modeled for all materials. The numbers of elements and nodes are presented in Table 1. All parameters of the materials were adopted from reference[28].

To analyze the displacement of the novel abutment under load, we applied a vertical force of 5 N to the abutments at a speed of 0.2 mm/s and recorded their displacement behavior. With a displacement control of 0.21 mm, we measured the maximum stress within the implant. To simulate occlusal conditions, we applied a force of 118.2 N at an angle of approximately 75° to the occlusal plane on the abutments and evaluated the resulting stress distribution.

Table 1 The types and numbers of different component elements.

Components	Element type	Element numbers	Node numbers
Abutment (commercial implant)	C3D10M	1394	2496
Abutment (novel implant)	C3D10M	6984	11,165
Fixture	C3D10M	18,136	27,824
Coping	C3D10M	2869	5323
Buffer	C3D10M	787	1620
Cortical bone	C3D10M	4707	8224
Cancellous bone	C3D10M	13,912	20,698

Results

Physical properties of composite hydrogels

The stress—strain curve of the composite hydrogels exhibited two distinct characteristics. The initial stage (strain 0 %—45 %) demonstrated a non-linear response, while the later stage (strain 45 %—50 %) displayed a more linear trend. Consequently, in this study, the slope of the linear segment within the 45 %—50 % strain range was used to determine the compressive modulus of the two composite hydrogels. The compressive modulus was calculated by substituting the stress—strain values from the linear segment into Formulas 1.1 and 1.2. The compressive moduli for HS and HSP were found to be 0.41 MPa and 1.21 MPa, respectively. The Pearson correlation coefficient between the HS and HSP groups was 0.95.

According to the creep test results, the height of the specimen decreased as the duration of the applied load increased. For both materials, the reduction in height stabilized and smoothed out at 180 s. An equilibrium state was achieved after the load was maintained for 1 h. At equilibrium, the height reductions for the HSP and HS test specimen groups were 2.35 ± 0.47 mm and 3.87 ± 0.21 mm, respectively.

To estimate the permeability of the composite hydrogels, we compared the theoretical results using the mathematical model (Equation (1.4)) and the experimental creep test results. It was observed that both the HS and HSP groups exhibited a good correlation between the experimental and theorectical curves. The biphasic material parameters of the hydrogel specimens were obtained with the curve fitting. For the HS group, the aggregate modulus was 0.0135 ± 0.003 MPa, the liquid permeability was $720.84 \pm 249.61 \times 10^{-12}$ m^4/N, and $M = 15$. For the HSP group, the aggregate modulus was 0.031 ± 0.004 MPa, the liquid permeability was $172.8 \pm 81.68 \times 10^{-12}$ m^4/N, and $M = 20$.

Mechanical behavior of composite hydrogels with FEA

The displacement results for various mechanical properties of the hydrogel composites are shown in Fig. 3. As the permeability of the materials increased, a steeper slope was observed during the compression phase. This phenomenon could be attributed to the rapid expulsion of liquid, which was quickly supported by the solid matrix. During the unloading phase, lower permeability resulted in a longer duration to return to the initial position. The HSP group exhibited behaviors more similar to those of natural teeth compared to the HS group (Fig. 3a and b).

The results showed that the groups with the thicknesses of 0.3 mm and 0.9 mm exhibited unstable displacement stagnation during compression. The groups with thicknesses of 1.8 mm and 3 mm began to exhibit the characteristics of biphasic porous elastic materials (Fig. 3c). During the compression stage, an initial load was supported by a large amount of liquid loss, resulting in instantaneous displacement. Subsequently, the solid matrix itself bore this load due to its strength, causing the displacement to decrease gradually until reaching an equilibrium state. With an increase in thickness, the displacement of the cushioning material increased and extended the time to reach the maximum deformation, enhancing its buffering capacity. The unloading phase also showed similar behaviors, with the characteristics of this biphasic material becoming more prominent with increasing thickness.

In Fig. 3d, it is evident that the softer the solid matrix, the larger the compression modulus and the greater the displacement during compression under controlled permeability and loading conditions. When the compression modulus reached 0.4 MPa, the displacement achieved the target value of 0.2 mm.

Displacement and stress distribution of implants

With constant loads on the implant model, the implant presented sinking behavior in both groups. The sinking performance could be divided into two phases: quick sinking and maintaining. With unloading, the implants rapidly returned to their original position (Fig. 4a). However, the commercial implant did not present detectable movement in this analysis. With the displacement of the abutment set as 0.21 mm, the force on the commercial implants presented a steeper slope with displacement. In contrast, the novel implants with buffer materials presented a small

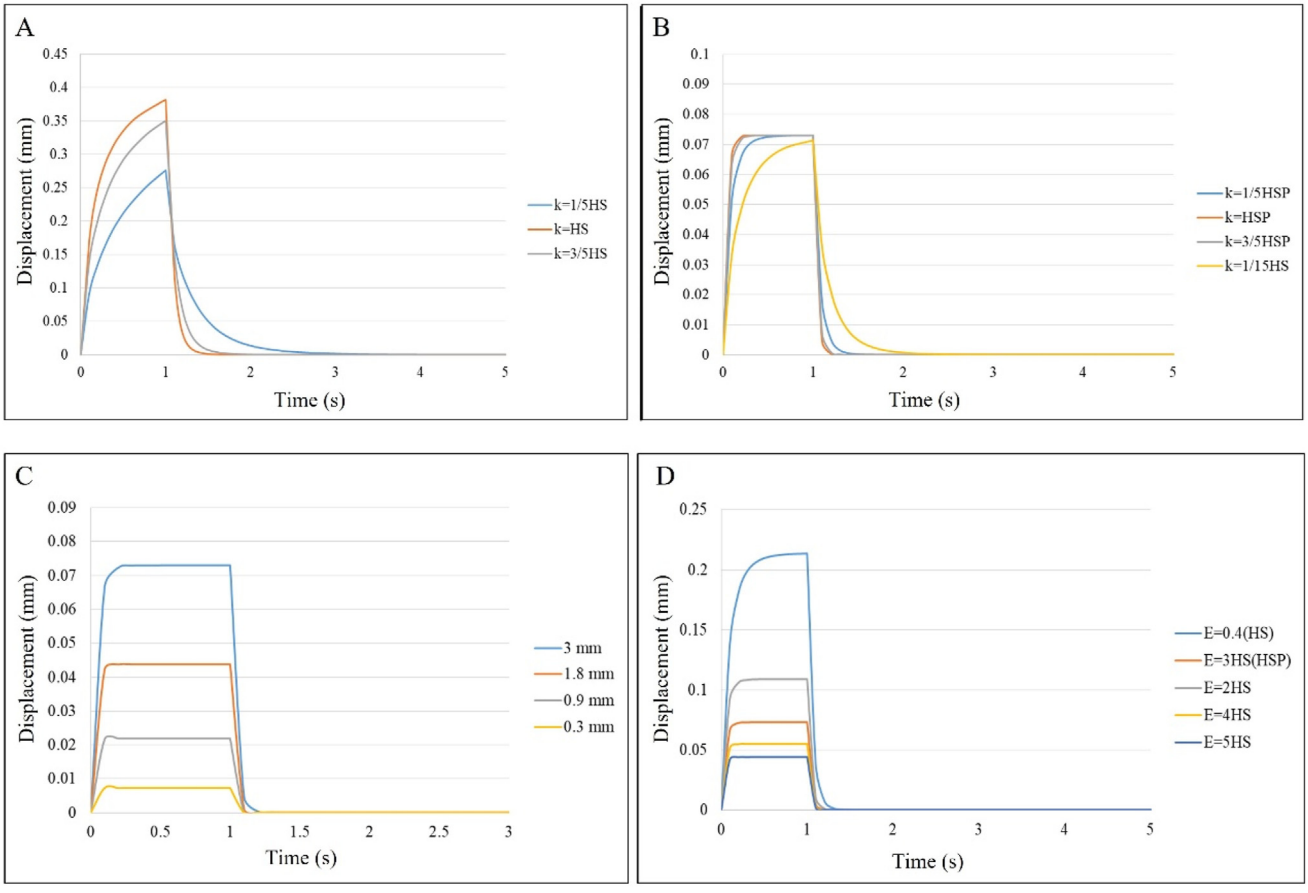

Figure 3 The results of various mechanical properties of the hydrogel composite material on displacement with finite element analysis. The impact of different permeabilities of the HS groups (A) and the HSP groups (B), as well as the impact of material thickness (C) and compression modulus (D) of the HSP groups, were presented.

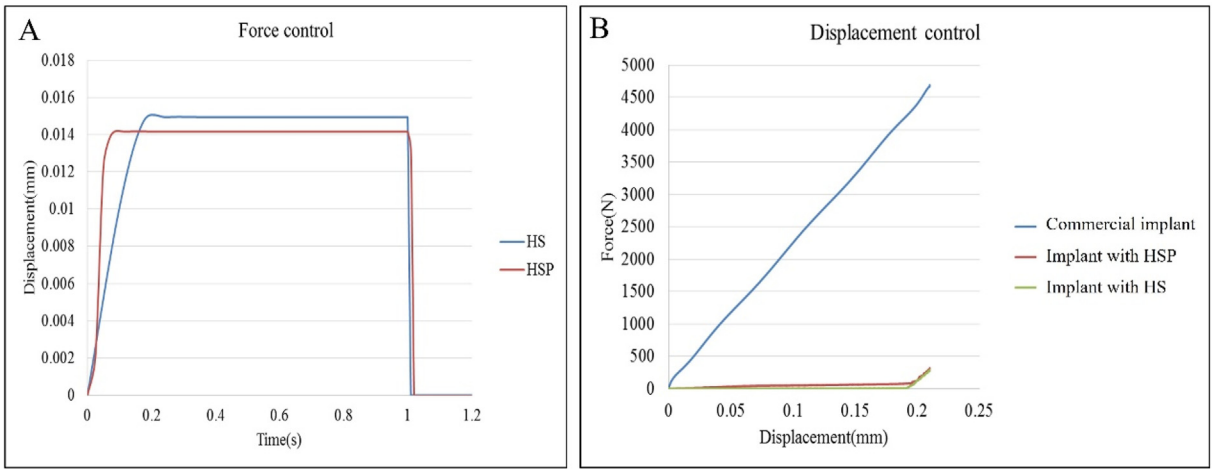

Figure 4 Finite element analyzed results for implants displacement with loading. (A) The displacement of the HS and HSP implants with force control. (B) The force on the HS and HSP implants and the commercial implant with displacement control.

force generated in the first displacement of 0.2 mm. When exceeding the allowable displacement of the structure, the force increased rapidly, similar to the commercial implants (Fig. 4b).

In Fig. 5a, the stress distribution of the surrounding tissue with different implants under oblique forces presented similar performance for the three groups. In the two novel implant groups, force transmission started with the contact of the upper cover thread on the buccal side and transferred the force from the buccal side to the lingual side. Partial force was absorbed through the buffer materials. Finally, the force was transmitted to the surrounding alveolar bone through the implant threads. By observing the stress distribution of alveolar bone under oblique loading through the FEA, the stress on the implant was concentrated on the first thread of the implants, with the maximum equivalent von Mises stress of approximately 90.12 MPa for the commercial implant group, 80.8 MPa for the HS group, and 77.9 MPa for the HSP group. As compared to the commercial implant group, the stress values of the HS and HSP groups decreased by 10.3 % and 13.6 %, respectively. When observing the stress at the lower thread implant body, the maximum equivalent von Mises stress was about 37.5 MPa for the commercial group, approximately 39.36 MPa for the HS group of the buffer implant, and around 36.56 MPa for the HSP group (Fig. 5b).

Discussion

Traditional dental implants primarily exhibit rigid body displacement when subjected to loading, largely due to the deformation of both the implant and the surrounding bone tissue. In contrast, the PDL connecting natural teeth to the alveolar bone allows for a greater displacement when natural teeth experience force. This mechanism promotes

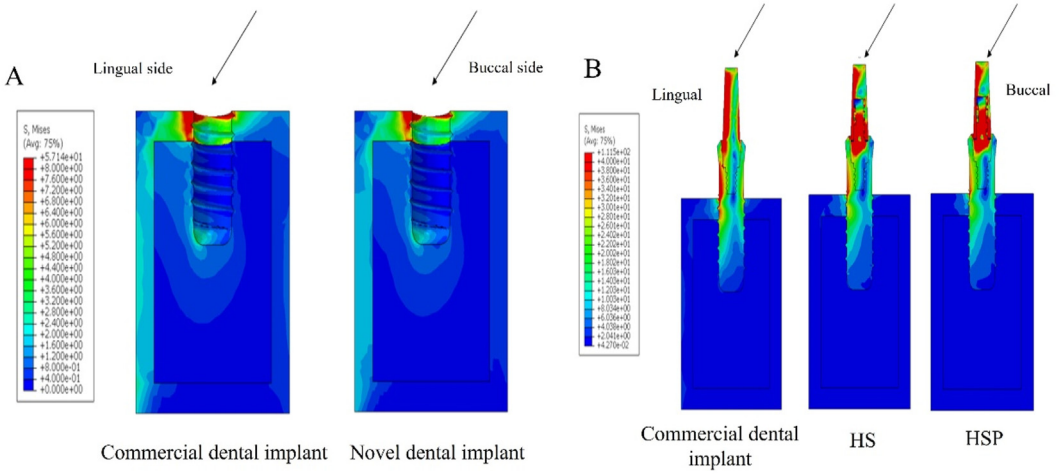

Figure 5 The finite element analyzed stress distribution on the surrounding bone and dental implant under oblique force with the commercial and novel implants. (A) The stress distribution on the surrounding bone showed similar performance between the commercial and novel dental implant groups. (B) The novel dental impalnts with the HS and HSP samples showed internal stress redistribution compared with the commercial dental implant.

more uniform stress distribution across all teeth in the mouth, thereby preventing individual teeth from experiencing the occlusal overload. Previous studies on the performance of the PDL under load have identified two phases: the first phase involves a linear movement, while the second phase demonstrates a non-linear behavior. Notably, the displacement of the implant model remains constant under sustained loading. During the unloading phase, the implant first rapidly returns to the half position and then slowly repositions to the original place.[12,13,15,29] Some scholars[15,17] have suggested that this mechanical behavior is due to the fluid and solid (collagen fibers) composite structure within the PDL. This study used novel composite hydrogels for dental implants to exhibit mechanical behaviors similar to the natural teeth with functional loading.

The PDL is a crucial stress-bearing tissue for the natural teeth. To accurately simulate the mechanical behavior of the PDL, the cushioning materials within dental implants must possess adequate mechanical strength to withstand the occlusal loads. Previous studies have shown that the compressive modulus of the PDL ranges from 0.07 to 1750 MPa.[30] The mechanical strength of the PDL varies significantly due to individual differences such as age, periodontal condition, and variations in tooth size and dentition. Additionally, differences in experimental designs and loading devices have contributed to variations in the results. In this study, composite hydrogels were applied and analyzed as cushioning materials for their functional properties. It was found that the compressive moduli of the two composite hydrogels were comparable to those of previously studied PDL. This finding suggests that the composite hydrogels exhibit a mechanical strength trend similar to that of the natural PDL, particularly in the solid phase. Furthermore, the HSP group demonstrated a higher compressive modulus, enabling it to withstand larger compressive loads.

According to the creep test results, the height of the specimens decreased by approximately 2—4 mm after the composite hydrogel was subjected to a fixed load for 1 h. The sinking behaviors presented the biphasic phenomenons. This finding suggests that when the composite hydrogel bears this load, it experiences an initial displacement due to the significant liquid loss, followed by the solid matrix of the hydrogel supporting the load until the internal pressure equilibrates with the fixed load, at which point the liquid flow ceases. This phenomenon resembles that of the natural PDL. The natural teeth undergo rapid initial displacement toward the root apex with slight movement when subjected to occlusal force, after which the occlusal load is evenly transmitted to the alveolar bone through the PDL.[26,29] This slight movement, known as the escape mechanism, could share the occlusal load with the adjacent natural teeth. This mechanism could protect teeth and implants from overloading and enhance the survival rate.[15,18] In 2014, our research group investigated the biomechanical behaviors of the dog teeth.[31] The result showed that the displacement of the tooth gradually decreases with a 500 g load. A larger displacement was immediately generated at the beginning of the loading to achieve a buffering effect (escape mechanism), and in the later stage of loading, the natural teeth gradually exhibited a supporting effect. When reaching equilibrium, the amount of displacement change was approximately 0.16 mm. In this study, the composite hydrogel exhibited a mechanical behavior similar to that of the PDL.

According to the analysis results (Fig. 3c), the HSP group exhibited the characteristics of the biphasic porous elastic materials with a thicknesses of 1.8 mm and 3 mm. In the loading stage, the instantaneous displacement was presented as the first phase due to the movement of liquid. The solid matrix bore the loading as the second phase and gradually decreased the displacement until reaching an equilibrium state. While the thickness of buffer materials increased, the buffer material presented more displacement and extended time to a maximum deformation. This indicates that thicker material exhibits more capability of buffering. The unloading stage also performed a similar behavior. With an increasing thickness, the characteristics of this biphasic material become more pronounced. Regarding the effect of permeability, the rate of displacement increases rapidly with increasing permeability of both composite hydrogels during the loading stage (Fig. 3a and b). A similar behavior was also shown in the unloading stage. The smaller the permeability, the longer it takes to return to the initial position. The discovery of the current study that the dual-phase material properties can affect the stiffiness variations of the composite hydrogel is similar to the previous studies.[27,32] They used a porous elastic body to describe the non-linear mechanical behavior of the PDL and investigated the effect of different permeabilities on its stiffiness relaxation response. Therefore, the permeability and thickness of the buffering material could affect the volume and time of displacement when applied to the dental implants.

This study evaluated the physical performance of artificial dental implants with the application of composite hydrogels inside with loading. We used the biphasic porous elastic model as the buffer materials for new artificial dental implants. In the constant loading phase, the new dental implant initially underwent instantaneous displacement and a gradual decrease in displacement. The results were similar to the natural teeth with the PDL.[12] However, the results of this study presented a different behavior compared to previous studies in the unloading phase. This could result from the buffer body size set in this study being too thin and leading to a rapid discharge of the liquid. Considering the impact on the dental implants with occlusal loading, both the HS and HSP groups could effectively reduce the maximum von Mises stress in the cortical bone and the implant. The HSP group performed better results. Both composite hydrogels could absorb and buffer the occlusal loading transmitted to the dental implant. Reduction of stress concentration on the dental implant can improve the long-term survival rate of the implants. Considering the impact on the alveolar bone, the von Mises stress on the surrounding cortical and cancellous bone showed the same distribution among the new artificial dental implants and traditional implants. This indicates that the modification of the abutment can maintain reliable performance of dental implants.

In this study, we adjusted the solid mechanical properties and the liquid permeability of composite hydrogels to simulate the movement characteristics of the PDL in the natural teeth. Our findings indicate that the biphasic nature

of solid and liquid components must be considered when implementing a buffering mechanism in implants to replicate the characteristics of the PDL. Future researches will explore the use of single materials or multiple mechanisms in this context.

Declaration of competing interest

The authors have no conflicts of interest relevant to this article.

Acknowledgments

This study was supported by grants 112-2221-E-027-010-MY3 from the National Science and Technology Council (NSTC), Taiwan.

References

1. Charyeva O, Altynbekov K, Zhartybaev R, Sabdanaliev A. Long-term dental implant success and survival-a clinical study after an observation period up to 6 years. *Swed Dent J* 2012;36:1—6.
2. Su MZ, Chang HH, Chiang YC, et al. Modeling viscoelastic behavior of periodontal ligament with non-linear finite element analysis. *J Dent Sci* 2013;8:121—8.
3. Hasegawa T, Kawabata S, Takeda D, et al. Survival of Branemark System Mk III implants and analysis of risk factors associated with implant failure. *Int J Oral Maxillofac Surg* 2017;46:267—73.
4. Sims NA, Gooi JH. Bone remodeling. Multiple cellular interactions required for coupling of bone formation and resorption. *Semin Cell Dev Biol* 2008;19:444—51.
5. Simonis P, Dufour T, Tenenbaum H. Long-term implant survival and success: a 10-16-year follow-up of non-submerged dental implants. *Clin Oral Implants Res* 2010;21:772—7.
6. Heinemann F, Hasan I, Bourauel C, Biffar R, Mundt T. Bone stability around dental implants: treatment related factors. *Ann Anat* 2015;199:3—8.
7. He Y, Fok A, Aparicio C, Teng W. Contact analysis of gap formation at dental implant-abutment interface under oblique loading: a numerical-experimental study. *Clin Implant Dent Relat Res* 2019;21:741—52.
8. Berkovitz BK. The structure of the periodontal ligament: an update. *Eur J Orthod* 1990;12:51—76.
9. Nanci A, Bosshardt DD. Structure of periodontal tissues in health and disease. *Periodontol* 2000 2006;40:11—28.
10. Jeon PD, Turley PK, Moon HB, Ting K. Analysis of stress in the periodontium of the maxillary first molar with a three-dimensional finite element model. *Am J Orthod Dentofacial Orthop* 1999;115:267—74.
11. Nikolaus A, Currey JD, Lindtner T, Fleck C, Zaslansky P. Importance of the variable periodontal ligament geometry for whole tooth mechanical function: a validated numerical study. *J Mech Behav Biomed Mater* 2017;67:61—73.
12. Qian L, Todo M, Morita Y, Matsushita Y, Koyano K. Deformation analysis of the periodontium considering the viscoelasticity of the periodontal ligament. *Dent Mater* 2009;25:1285—92.
13. Boldt J, Knapp W, Proff P, Rottner K, Richter EJ. Measurement of tooth and implant mobility under physiological loading conditions. *Ann Anat* 2012;194:185—9.
14. Tuna M, Sunbuloglu E, Bozdag E. Finite element simulation of the behavior of the periodontal ligament: a validated non-linear contact model. *J Biomech* 2014;47:2883—90.
15. Wang CY, Su MZ, Chang HH, et al. Tension-compression viscoelastic behaviors of the periodontal ligament. *J Formos Med Assoc* 2012;111:471—81.
16. Fill TS, Toogood RW, Major PW, Carey JP. Analytically determined mechanical properties of, and models for the periodontal ligament: critical review of literature. *J Biomech* 2012;45:9—16.
17. McCormack SW, Witzel U, Watson PJ, Fagan MJ, Groning F. Inclusion of periodontal ligament fibres in mandibular finite element models leads to an increase in alveolar bone strains. *PLoS One* 2017;12:e0188707.
18. Duyck J, Vandamme K. The effect of loading on peri-implant bone: a critical review of the literature. *J Oral Rehabil* 2014;41:783—94.
19. Fakhari A, Berkland C. Applications and emerging trends of hyaluronic acid in tissue engineering, as a dermal filler and in osteoarthritis treatment. *Acta Biomater* 2013;9:7081—92.
20. Cao Y, Wang B. Biodegradation of silk biomaterials. *Int J Mol Sci* 2009;10:1514—24.
21. Vincent LG, Choi YS, Alonso-Latorre B, Del Álamo JC, Engler AJ. Mesenchymal stem cell durotaxis depends on substrate stiffness gradient strength. *Biotechnol J* 2013;8:472—84.
22. Mehdi G, Belarbi A, Mansouri B, Azari Z. Numerical study of effect of elastomeric stress absorbers on stress reduction in bone-dental implant interface. *J Appl Oral Sci* 2015;23:87—93.
23. Chen YY, Chen WP, Chang HH, Huang SH, Lin CP. A novel dental implant abutment with micro-motion capability-development and biomechanical evaluations. *Dent Mater* 2014;30:131—7.
24. Chu CM, Huang HL, Hsu JT, Fuh LJ. Influences of internal tapered abutment designs on bone stresses around a dental implant: three-dimensional finite element method with statistical evaluation. *J Periodontol* 2012;83:111—8.
25. Genna F, Paganelli C, Salgarello S, Sapelli P. 3-D numerical analysis of the stress state caused by short-term loading of a fixed dental implant containing a" PDL-like" non-linear elastic internal layer. *Comput Model Eng Sci* 2003;4:405—20.
26. Silva P, Crozier S, Veidt M, Pearcy M. An experimental and finite element poroelastic creep response analysis of an intervertebral hydrogel disc model in axial compression. *J Mater Sci Mater Med* 2005;16:663—9.
27. Argoubi M, Shirazi-Adl A. Poroelastic creep response analysis of a lumbar motion segment in compression. *J Biomech* 1996;29:1331—9.
28. Bulaqi HA, Mashhadi MM, Safari H, Samandari MM, Geramipanah F. Effect of increased crown height on stress distribution in short dental implant components and their surrounding bone: a finite element analysis. *J Prosthet Dent* 2015;113:548—57.
29. Bergomi M, Cugnoni J, Galli M, Botsis J, Belser UC, Wiskott HWA. Hydro-mechanical coupling in the periodontal ligament: a porohyperelastic finite element model. *J Biomech* 2011;44:34—8.
30. Fill TS, Carey JP, Toogood RW, Major PW. Experimentally determined mechanical properties of, and models for, the periodontal ligament: critical review of current literature. *J Dent Biomech* 2011;2011:312980.
31. Chen YY. *Research and development of novel dental implant system with micro-Motion mechanism*. PhD thesis, National Taipei University of Technology Department of Mechanical Engineering: Taipei, 2014.
32. Favino M, Bourauel C, Krause R. A non-linear poroelastic model for the periodontal ligament. *Int J Comput Methods Eng Sci Mech* 2016;17:172—81.